Electronic Supplementary Material (ESI) for Journal of Materials Chemistry C.

Supporting Information

Luminescence analysis in heavy Mn^{2+}-doped $LaMgAl_{11}O_{19}$ phosphor: crystallographic site occupation and formation of Mn^{2+}-Mn^{2+} dimers

Chenyang Zhan[a,b,c,d], Haomiao Zhu,[a,b,c,d] Sisi Liang,[c,d] Yingping Huang,[c,d] Wendong Nie,[c,d] Zihao Wang,[c,d] and Maochun Hong*[a,b,c,d]*

a. School of Rare Earths, University of Science and Technology of China, Hefei, Anhui 230026, China

b. Ganjiang Innovation Academy, Chinese Academy of Sciences, Ganzhou, Jiangxi 341119, China

c. CAS Key Laboratory of Design and Assembly of Functional Nanostructures, Fujian Key Laboratory of Nanomaterials, Fujian Institute of Research on the Structure of Matter, Chinese Academy of Sciences, Fuzhou, Fujian, 350002, China

d. Xiamen Key Laboratory of Rare Earth Photoelectric Functional Materials, Xiamen Research Center of Rare Earth Materials, Haixi Institute, Chinese Academy of Sciences, Xiamen 361021, China

E-mail: zhm@fjirsm.ac.cn

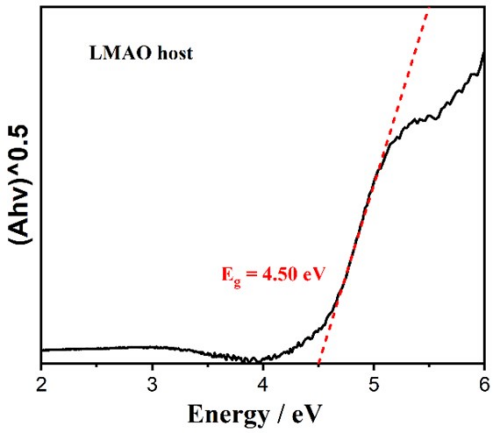

Fig. S1 The calculated bandgap value of the LMAO host was determined by the plot of [Ahv]^0.5 *versus* energy (eV).

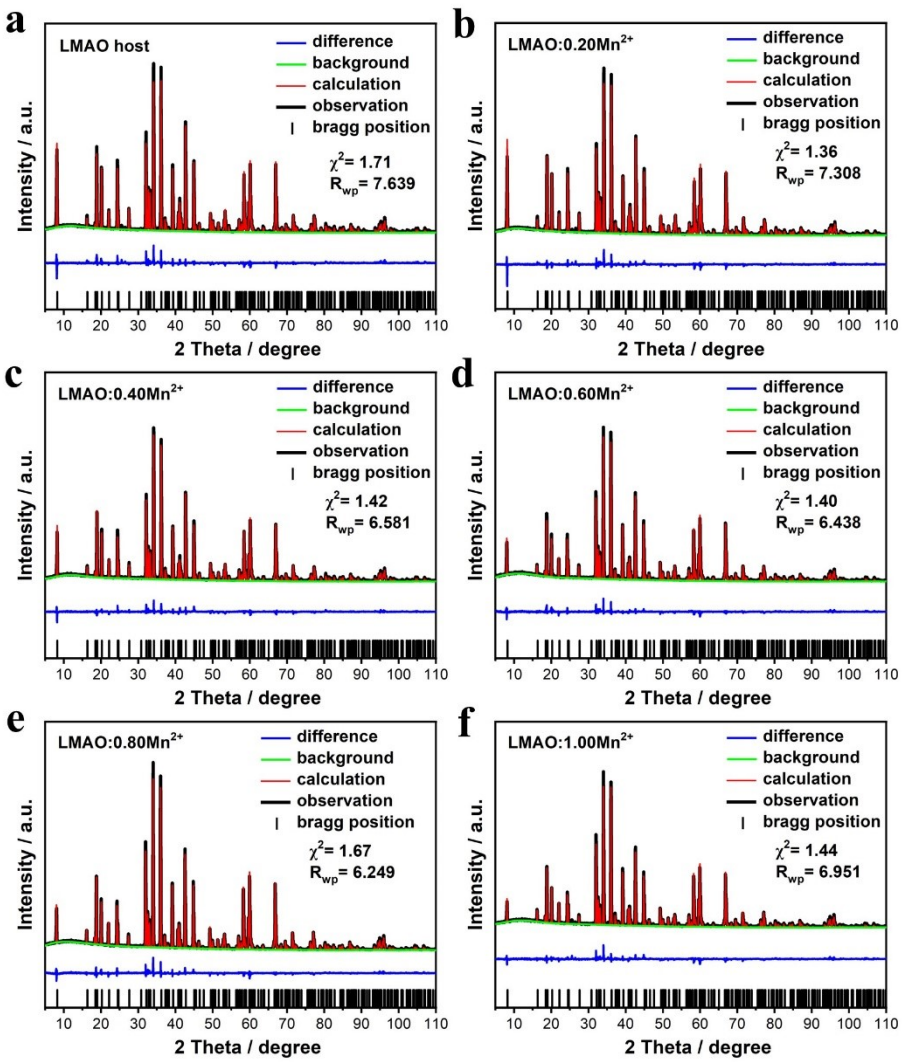

Fig. S2 Rietveld refinement of XRD patterns for LMAO: xMn^{2+} ($0 \leq x \leq 1.00$) phosphors.

Table S1. Crystallographic parameters for LMAO: xMn^{2+} ($0 \le x \le 1.00$) phosphors based on Rietveld refinement.

	x=0	x=0.20	x=0.40	x=0.60	x=0.80	x=1.00
Crystal system	hexagonal	hexagonal	hexagonal	hexagonal	hexagonal	hexagonal
Space group	P63/mmc	P63/mmc	P63/mmc	P63/mmc	P63/mmc	P63/mmc
a = b (Å)	5.5902	5.5931	5.5959	5.5974	5.5985	5.6024
c (Å)	21.9605	21.9729	21.9863	22.0064	22.0192	22.0366
α = β (°)	90	90	90	90	90	90
γ (°)	120	120	120	120	120	120
V (Å^3)	594.339	595.280	596.323	597.099	597.785	599.003
R_{wp} (%)	7.639	7.308	6.581	6.438	6.249	6.951
χ^2	1.71	1.36	1.42	1.4	1.67	1.44

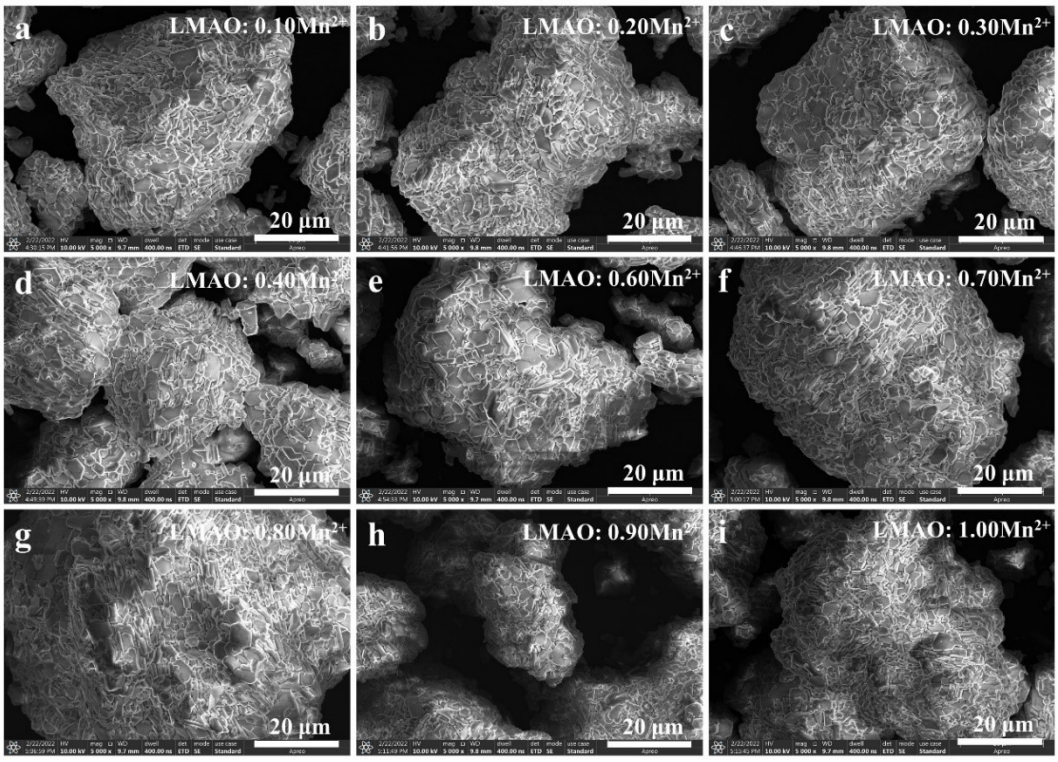

Fig. S3 The typical SEM images of the LMAO: xMn^{2+} ($0.10 \le x \le 1.00$) phosphors at

different magnifications.

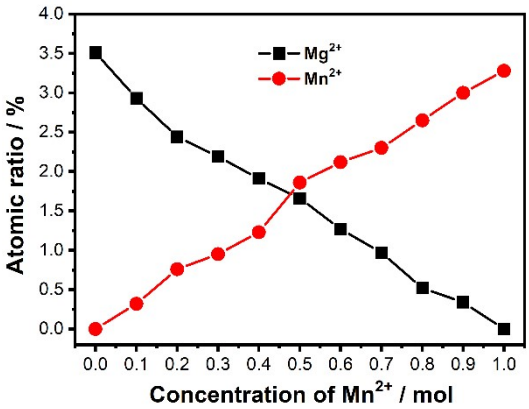

Fig. S4 The atomic ratios of Mg and Mn elements in LMAO: xMn^{2+} ($0 \le x \le 1.00$) phosphors were determined by EDS.

Table S2. Atomic ratios among La, (Mg+Mn), Al, O elements at different Mn^{2+} doping concentrations in LMAO: xMn^{2+} ($0 \le x \le 1.00$) phosphors.

x(mol)	La	(Mg+Mn)	Al	O
0	1	1.0204	11.2151	15.8343
0.1	1	1.0515	11.6817	18.4244
0.2	1	1.0188	11.2759	18.0533
0.3	1	1.0561	11.6337	19.3102
0.4	1	1.0064	11.1987	18.8462
0.5	1	1.1095	12.1237	21.1025
0.6	1	1.2055	12.1815	19.8562
0.7	1	1.0399	11.4356	17.1994
0.8	1	1.0900	11.6233	19.6200
0.9	1	1.0064	11.3460	18.3905
1	1	1.0152	11.9605	16.4195

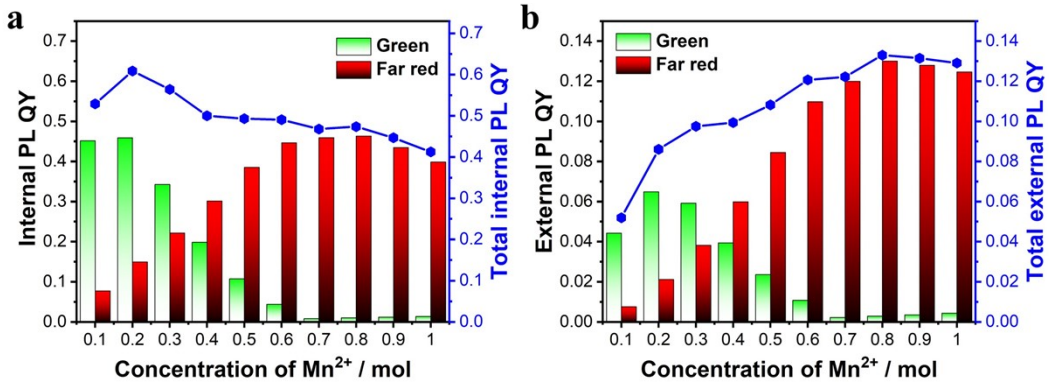

Fig. S5 The variation of the internal/external PL QYs with Mn^{2+} doping concentration in LMAO: xMn^{2+} ($0 \le x \le 1.00$) phosphors under the excitation of 450 nm.

Table S3. The internal PL QYs, external PL QYs, and absorption efficiency (AE) vary with the doped concentration of Mn^{2+} in LMAO: xMn^{2+} ($0 \le x \le 1.00$) phosphors.

x(mol)	AE	Internal PL QYs (green)	Internal PL QYs (far red)	External PL QYs (green)	External PL QYs (far red)
0.1	0.0980	0.4517	0.0775	0.0443	0.0076
0.2	0.1414	0.4591	0.1496	0.0649	0.0212
0.3	0.1727	0.3427	0.2216	0.0592	0.0383
0.4	0.1986	0.1987	0.3016	0.0395	0.0599
0.5	0.2193	0.1079	0.3854	0.0237	0.0845
0.6	0.2458	0.0440	0.4469	0.0108	0.1098
0.7	0.2611	0.0086	0.4595	0.0022	0.1200
0.8	0.2807	0.0104	0.4634	0.0029	0.1301
0.9	0.2942	0.0121	0.4348	0.0036	0.1279
1	0.3129	0.0139	0.3985	0.0044	0.1247

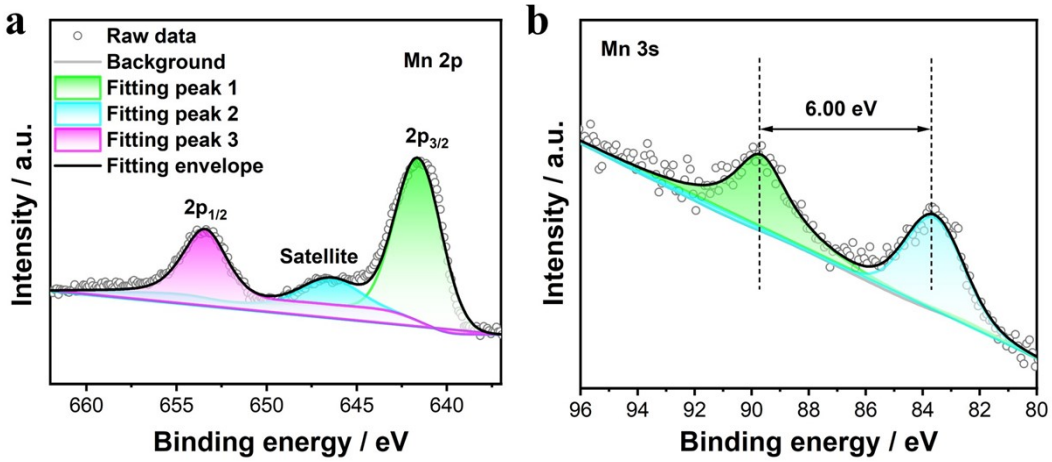

Fig. S6 High-resolution XPS spectra of Mn 2p and Mn 3s in LMAO: 1.00Mn^{2+} phosphor.

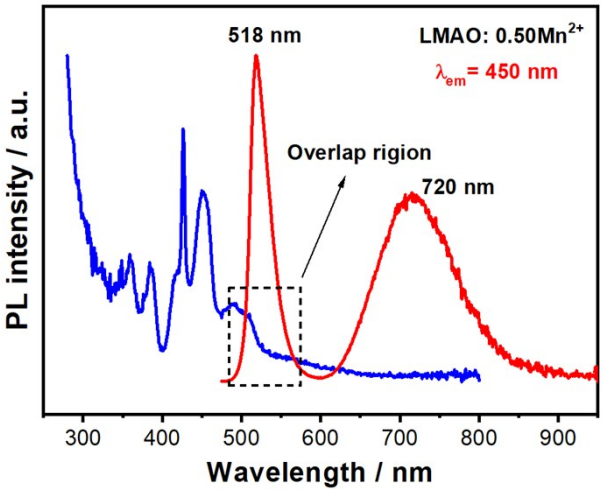

Fig. S7 The diffuse reflectance spectra and PL spectra of LMAO: 0.50Mn^{2+} phosphor. The dashed line shows the absorption spectrum of the far-red emission band overlaps with the PL spectrum of the green emission band in the region of 470 to 540 nm.

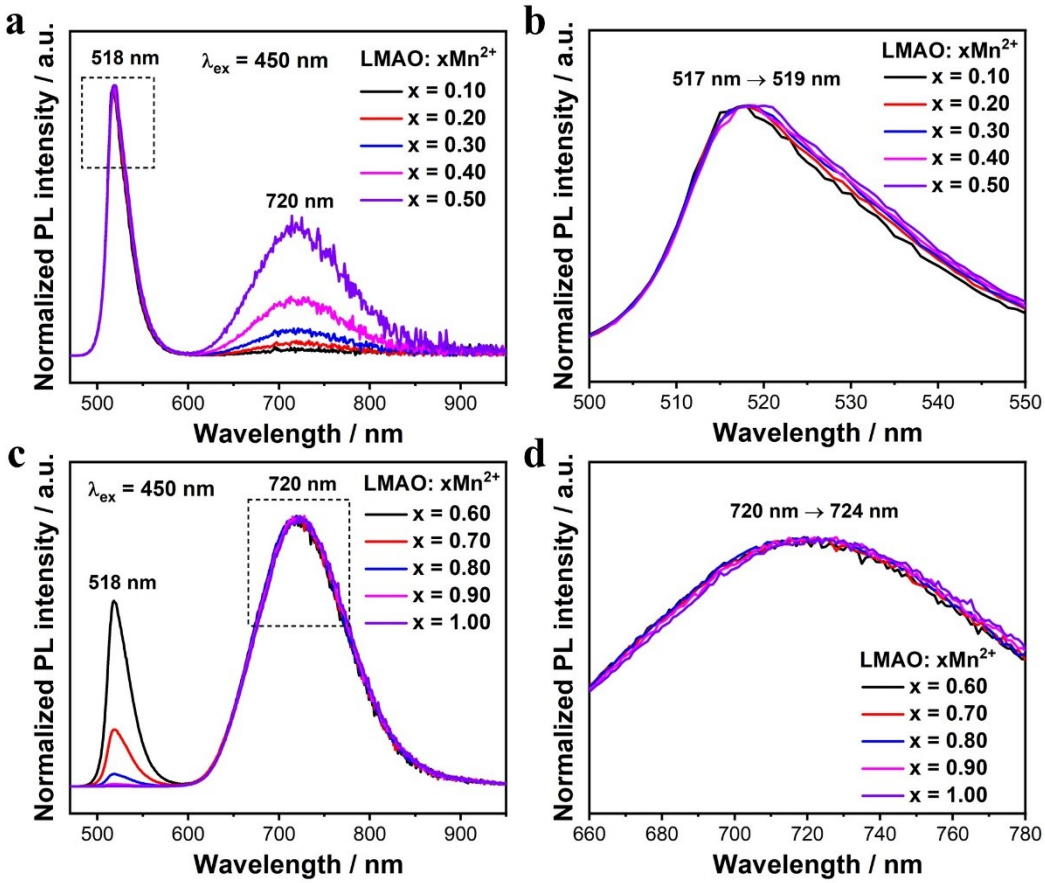

Fig. S8 The normalized PL spectra of LMAO: xMn^{2+} ($0 \le x \le 1.00$) phosphors.

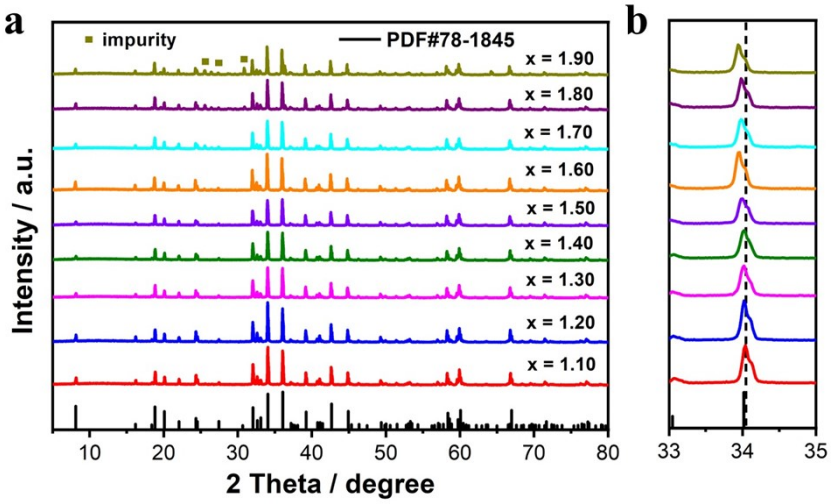

Fig. S9 XRD patterns of LMAO: xMn^{2+} ($1.10 \le x \le 1.80$) phosphors and the enlarged patterns in the region of 33°–35°.

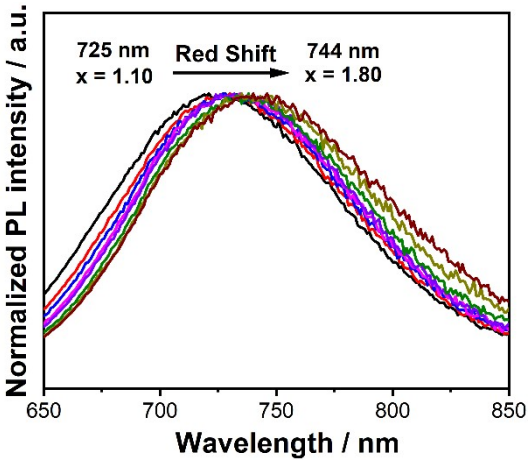

Fig. S10 The normalized PL spectra of LMAO: xMn^{2+} ($1.10 \leq x \leq 1.80$) phosphors upon 450 nm excitation.

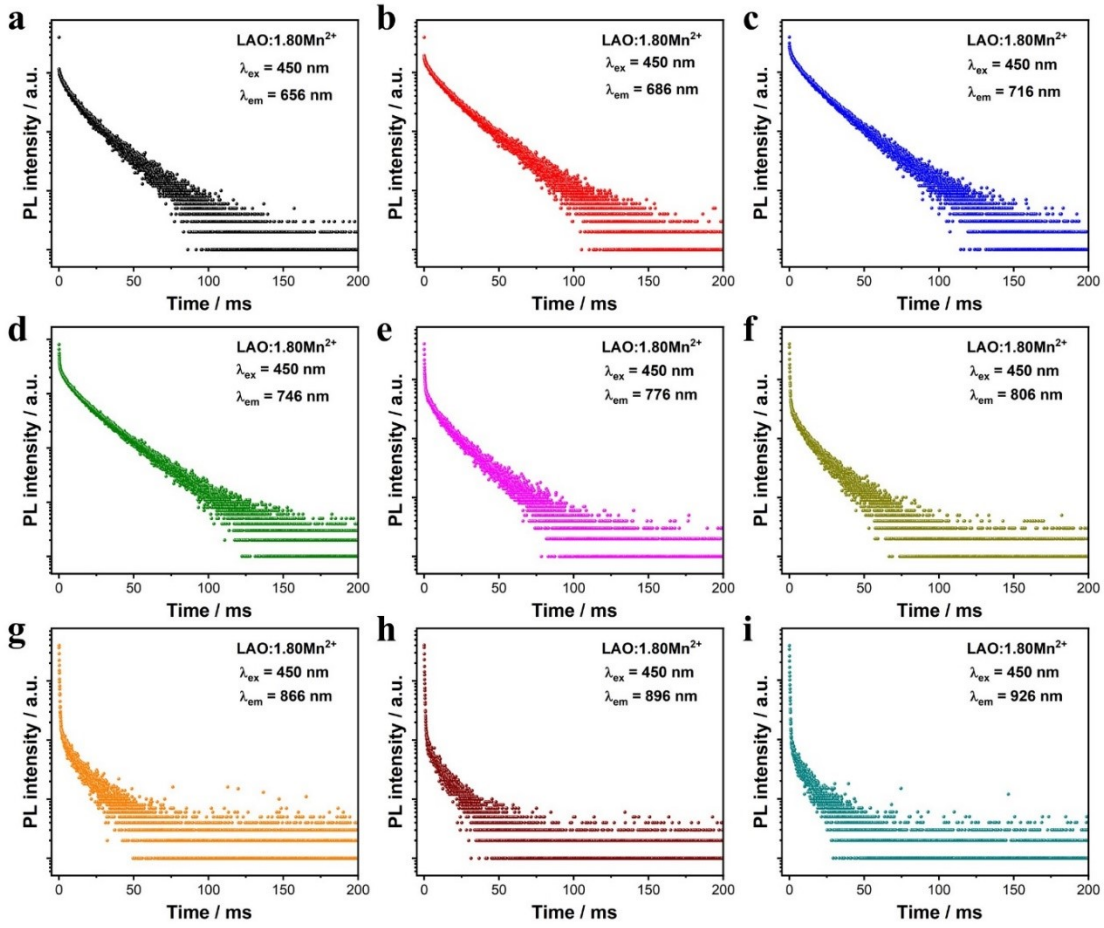

Fig. S11 The PL decay curve of Mn^{2+} in LMAO: $1.80Mn^{2+}$ phosphor when monitored the emission wavelength in the range from 656 nm to 926 nm.

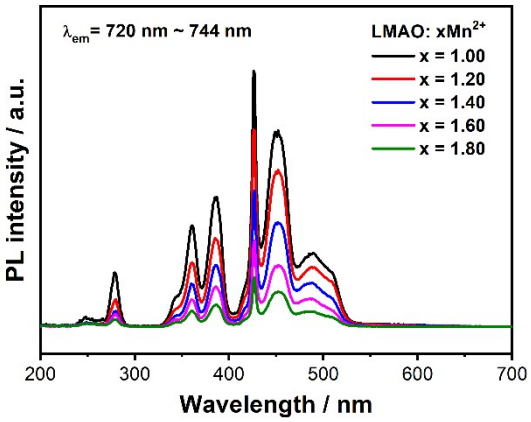

Fig. S12 The excitation spectra of LMAO: xMn^{2+} ($1.00 \leq x \leq 1.80$) phosphors.

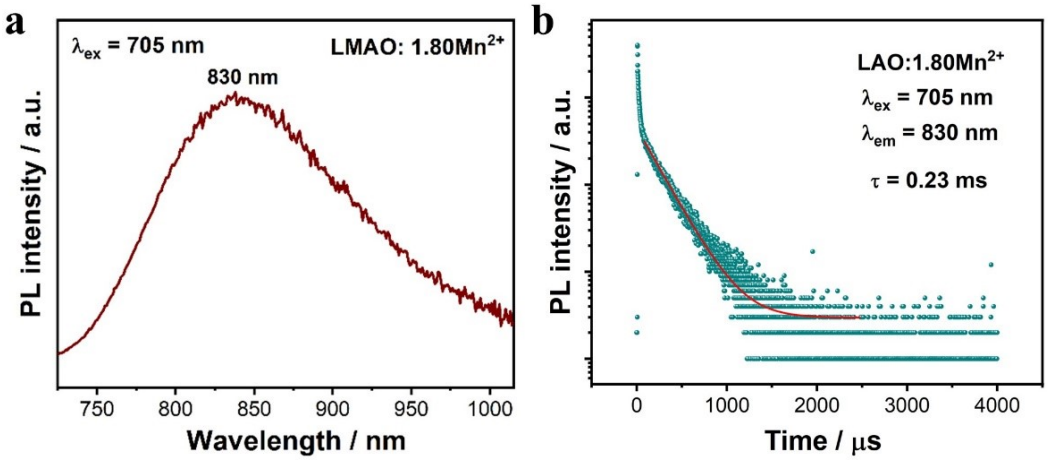

Fig. S13 a) The PL spectrum of LMAO: $1.80Mn^{2+}$ phosphor and b) The PL decay curve of Mn^{2+} in LMAO: $1.80Mn^{2+}$ phosphor when excited at 705 nm.

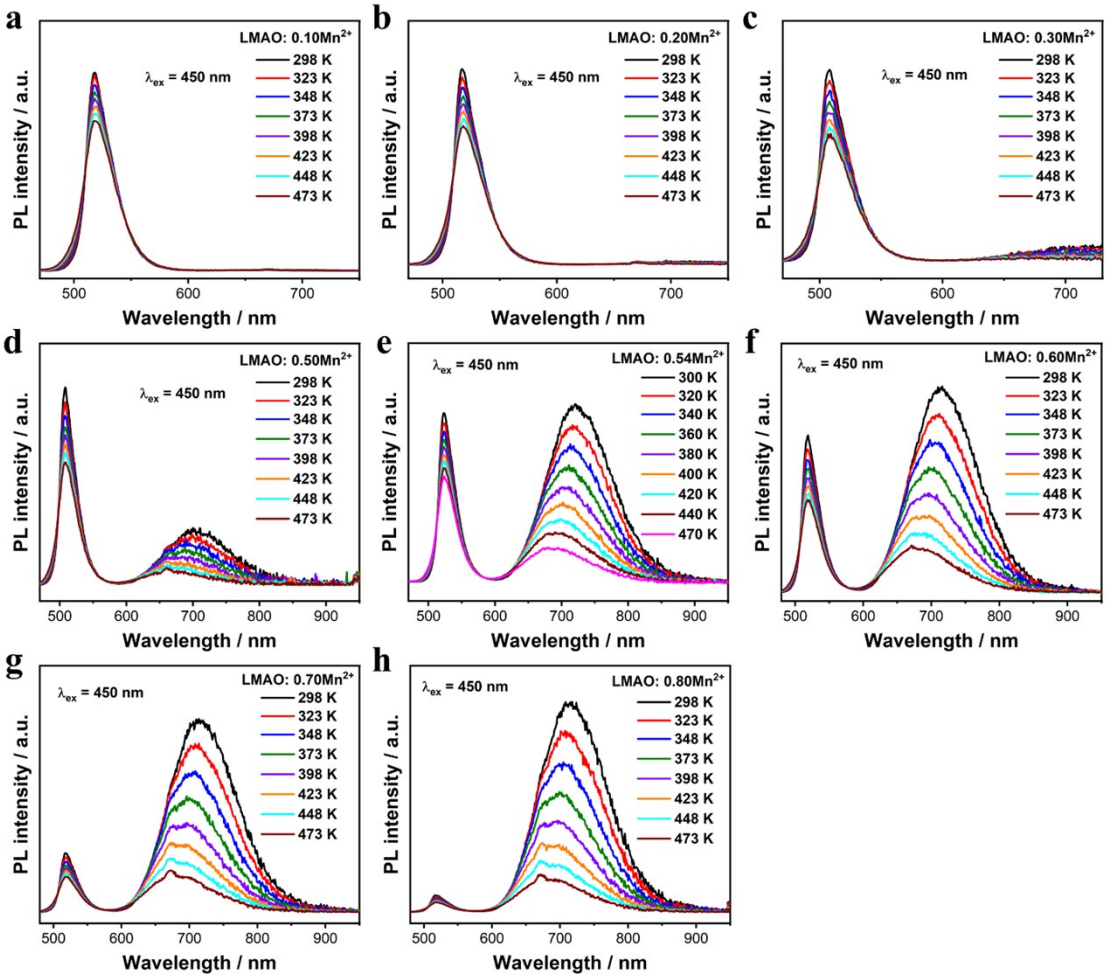

Fig. S14 Temperature-dependent PL spectra of LMAO: xMn^{2+} ($0.10 \leq x \leq 0.80$) phosphors under 450 nm excitation in the temperature of 298 – 473 K with a temperature interval of 25 K.

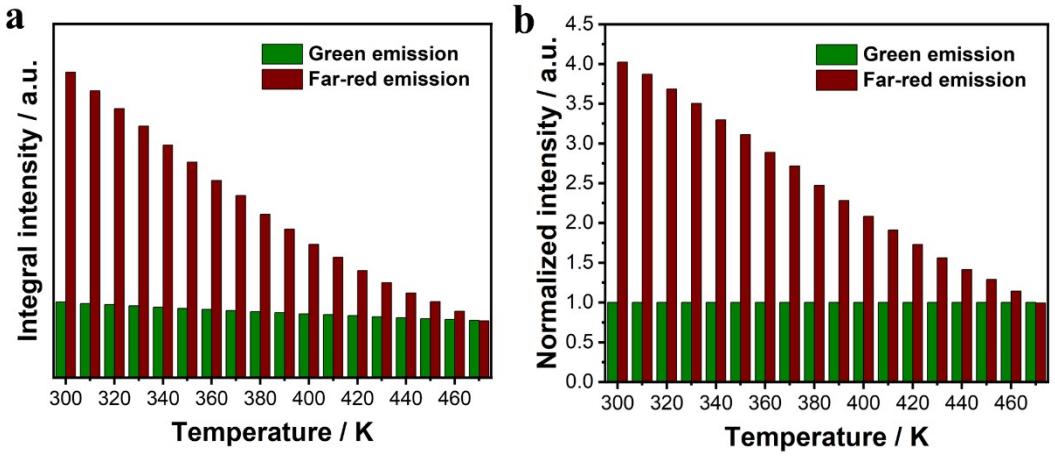

Fig. S15 The temperature dependent histogram of the emission intensity for green and far-red emission in LMAO: $0.54Mn^{2+}$ phosphor. a) integral intensity. b) by normalizing the green emission intensity.